Ocean Systems Engineering, *Vol. 11, No. 2 (2021) 123-140*
DOI: https:// doi.org/10.12989/ose.2021.11.2.123

Study of added resistance and seakeeping of KVLCC2 in waves with and without propeller

Hassiba Ouargli* and Benameur Hamoudi

Aero-hydrodynamic Laboratory (LAHN), Department of Maritime Engineering, University of Science and Technology of Oran MB, Oran 31000, Algeria

(Received July 20, 2020, Revised March 30, 2021, Accepted April 22, 2021)

Abstract. Numerical simulation of a full-scale ship model, KVLCC2, has been conducted applying the Reynolds Averaged Navier-Stokes (RANS) approach using the STARCCM+ commercial computational fluid dynamics (CFD) software to calculate total resistance, seakeeping and Pitch Moments. Results are obtained for the speed of 15.5 Knots under different sea conditions (calm water, regular waves and irregular waves), The total resistance calculated for the KVLCC2 ship hull in calm water is in a good agreement with the results from experiments and the results for motion (heave and pitch) and added resistance in waves were compared to numerical and experimental findings from previous research with good agreement. In addition to wave excitations, the full-scale ship model was subjected to propeller excitations using the virtual disk model from the CFD software. The body force propeller method, which simplified the full propeller characteristic of the KVLCC2 into a resultant body force, is applied to the virtual disk model. Results are compared with results from the hull-only model. A comparison of the wake results with previous work is also presented.

Keywords: CFD; free surface flow; pitch moment; heave; pitch; total resistance

1. Introduction

Computational fluid dynamics (CFD) has largely supplanted experimentation in both industry and research due to its reliability, lower time consumption, and significantly lower cost. The Korea Research Institute for Ships & Ocean Engineering (KRISO, formerly known as MOERI) developed the KVLCC2 model, which is one of the benchmark hulls used by researchers. KVLCC2 is the second model of KVLCC where experiments have been performed in the towing tank to obtain wave field and total resistance. This work presents a study of total resistance of KVLCC2 in calm water and added resistance, motions (heave and pitch), and pitch moment in response to head waves, in addition to a study of these responses in presence of propeller excitations using the commercial software STARCCM+.

1.1 Background

*Corresponding author, Ph.D., E-mail: hassiba.ouargli@gmail.com

http://www.techno-press.org/?journal=ose&subpage=7 ISSN: 2093-6702 (Print), 2093-677X (Online)

Research studies have long used potential flow theory to solve the inviscid flow equations. However, for the presented application, the viscous effects are significant and must be taken into account, which can be afforded by a wide range of CFD models and tools. To check the validity of these tools, different ship models are designed to be studied (e.g., KCS container ship, KVLCC2, or US-DTMB); these have modern hull shapes with bulbous bows and transom stern.

Fluid-Structure interaction is one of the most challenging marine industry problems and is studied by coupling RANS/CFD with Finite Element software. The coupling can be done by several methods, such as the one-way, two-way, weak, and strong coupling. (Lakshmynarayanana *et al.* 2015) used two-way coupling to study ship motion and flexible model response in regular head waves for the 3-D barge hull modelled as beam (a classical idealization of ship hull structures). This was also used by ((Kim and Kim 2014) to model ship springing and whipping with a combination of the Rankine panel method (3-D) and structural models, beam-element (1-D), and shell-element (3-D). These two phenomena were also studied by (Seng *et al*. 2014) using the OpenFOAM CFD software with a flexible body solver on a barge, and the results were compared to the experiments. (Kim *et al*. 2014) compared model tests of springing, whipping, and fully-coupled hydroelastic numerical model for a 10000 TEU containership. The contribution of these two phenomena to the fatigue of marine vessels is considerable and has been studied by (Storhaug 2014), who focused on fatigue and loading of container ships and discussed model results and full-scale measurements from DNV. Experiments have also been conducted for this kind of research: (Hong and Kim 2014) made model tests on large ship hulls in waves; full-scale measurements of vibration damage due to springing and whipping at operational conditions for large modern ship hulls has also been presented (Barhoumi and Storhaug 2014).

In the 2nd ITTC-ISSC (2014) joint workshop, a benchmark test of the codes studying the seakeeping performance of ships was carried out (Kim and Kim 2016), in their paper included and compared the data from participants studying the heave, pitch, and vertical bending moment of the 6750-TEU containership with the flexible model tested by KRISO. (Kim *et al*. 2017) studied ship motion and added resistance prediction for KVLCC2 in head seas for different ship speeds using numerical results obtained from URANS CFD and 3-D potential methods in regular waves, which added resistance and vertical ship motion. The KVLCC model was studied through experimental assessment by (An *et al*. 2014); the objective of this study was to demonstrate the effectiveness of using outer-layer vertical blades in ship models, and the authors achieved a reduction of 2.15-2.76% in the coefficient of total resistance (C_{TM}) at model scale.

In this study, the 3-D turbulent unsteady flow around KVLCC2 is investigated using finite volume method with the k-ε standard model, hexahedral grid, and dynamic fluid body interaction (DFBI) model that considers the hull as a rigid body (i.e., hull's local deformation does not affect the fluid domain). The commercial software STAR CCM+ version 12.02.011 from CD-ADAPCO (now SIEMENS) was used. The KVLCC2 (3-D) model was studied in full scale. The calm water total resistance results are the first obtained for verification study of the numerical model before calculation of motion and Pitch Moment of the ship hull in head seas with addition to propeller excitation.

2. Formulation

The fluid in the continuous viscous domain is modelled as a mixture of two fluids, water and air, and for both of these, the same RANS equations are used. The fixed coordinate system (o, x, y, z) is

used, where *x* is the longitudinal direction at the free surface directed to the bow of the ship, *z* is the upward vertical direction at the aft perpendicular of the ship, and *y is* perpendicular to the latter in the portside direction. Gravity is considered the only force acting on the particle and is vertically directed along *z*. The incompressible steady-state RANS equations, as given in (Larsson and Raven 2010), will be in component form

$$\begin{aligned}
&\frac{\partial}{\partial x}(\rho u^2 + p) + \frac{\partial}{\partial y}(\rho uv) + \frac{\partial}{\partial z}(\rho uw) = (\frac{\partial \tau_{xx}}{\partial x} + \frac{\partial \tau_{xy}}{\partial y} + \frac{\partial \tau_{xz}}{\partial z}) \\
&\frac{\partial}{\partial x}(\rho uv) + \frac{\partial}{\partial y}(\rho v^2 + p) + \frac{\partial}{\partial z}(\rho uw) = (\frac{\partial \tau_{yx}}{\partial x} + \frac{\partial \tau_{yy}}{\partial y} + \frac{\partial \tau_{yz}}{\partial z}) \\
&\frac{\partial}{\partial x}(\rho uw) + \frac{\partial}{\partial y}(\rho vw) + \frac{\partial}{\partial z}(\rho w^2 + p) = (\frac{\partial \tau_{zx}}{\partial x} + \frac{\partial \tau_{zy}}{\partial y} + \frac{\partial \tau_{zz}}{\partial z}) - \rho g
\end{aligned} \tag{1}$$

In Eq. (1), *u, v,* and *w* are Velocity components, *P* is the mean pressure + $\frac{2}{3}\rho k$, ρ is the density, g is the acceleration due to gravity, and τ_{ij} is a stress tensor defined by

$$\tau_{ij} = (\mu + \mu_T)(\frac{\partial u_i}{\partial x_j} + \frac{\partial u_j}{\partial x_i}) \tag{2}$$

In Eq. (2), μ is the dynamic viscosity, μ_T is the turbulent dynamic viscosity, and k is the turbulent kinetic energy. For incompressible fluids, the equation of continuity solves the RANS equations by the theorem of the conservative transport of mass as follows

$$\frac{\partial u}{\partial x} + \frac{\partial v}{\partial y} + \frac{\partial w}{\partial z} = 0 \tag{3}$$

For the ship motion, the basic equation is expressed as follows

$$M\,\ddot{\vec{X}}(t) + C\,\dot{\vec{X}}(t) + K\vec{X}(t) = \sum \vec{F}(t) \tag{4}$$

In Eq. (4), M is the mass matrix, C is the damping matrix, K is the stiffness matrix, $\vec{X}(t)$ is the displacement vector, and $\vec{F}(t)$ is the external forces expressed by the fluid domain on the structure.

3. Methodology

3.1 Geometry and sea conditions

The main geometric characteristics of the KVLCC2 hull used in this study are presented in the Table 1 and Fig. 1.

The design speed of KVLCC2 is 15.5 Knots (7.9739 m/s). For both water and air, aerodynamic forces are neglected, and the ship hull is subjected to head seas for both calm water and wave simulations and left free to move in vertical z direction and y rotation (2-DOF). Table 2 presents all the sea conditions in this study.

Table 1 KVLCC2 Dimensions

Length over all, LOA (m)	333.6
Length of water line, LW (m)	325.5
Length between perpendiculars, LBP (m)	320.0
Beam, B (m)	58.0
Depth, D (m)	28
Draft, T (m)	20.8
Longitudinal centre of buoyancy from the aft perpendicular, LCB (m)	171.136
Volumetric displacement, Δ (m^3)	312622
Hull wetted surface, S (m^2)	27194.0
Speed, v	15.5 knots
Froude number, Fr	0.142
Block coefficient, CB	0.8098
Vertical centre of gravity from keel, KG (m)	18.56
LCG (%), fwd +	3.48

Table 2 Wave conditions

	Case N°	Speed (Knots)	ω_e (rad/s)	T (s)	λ (m)	H (m)	Propeller Disk RPM
Calm water	1	15.5	-	-	-	-	-
	1*						10
	1**						70
	1***						76
Regular wave	2	15.5	0.124	8.097	264.494	4.424	-
	2*	15.5	0.124	8.097	264.494	4.424	10
Regular wave	3	15.5	0.103	9.704	345	5.75	-
	3*	15.5	0.103	9.704	345	5.75	10
Regular wave	4	15.5	0.085	11.81	384	6.4	-
	4*	15.5	0.085	11.81	384	6.4	10
				Tp (s)	γ	**H_S (m)**	
Irregular wave JONSWAP	5	15.5	-	14.28	3.3	9	-
	5*	15.5	-	14.28	3.3	9	10

* with 10 RPM
** with 70 RPM
*** with 76 RPM

Fig. 1 KVLCC2 ship hull

3.2 Numerical method

The $k-\varepsilon$ standard turbulence model was selected for this study. This model has proven accurate for this kind of calculations because of its computational time saving compared to other models; this makes it popular for use in industry.

The free surface around the hull in calm water and in waves is predicted using the volume of fluid (VOF) method, which is a tool to determine the phase contact between two different fluids (multiphase flows), and for this local interface, refinements of the grid are applied to accurately capture the volume fraction of fluids.

The CFD simulations in this paper use RANS approach, applying the segregated flow model, and our discretisation term is a second-order upwind scheme with a SIMPLE algorithm. For regular waves, 5th-order theory was chosen and JONSWAP spectrum for irregular waves.

The DFBI model was used to better simulate ship behaviour. The ship hull is free to move with two degrees of freedom (heave and pitch motions). This model enables calculation of the exciting fluid forces on the hull. In STAR CCM+, the ship hull is assumed to be a rigid body for calculation of forces and hydrodynamic loads, and the response is heave, pitch, and pitch moment; this approach is extremely computationally demanding with various simplifications. In addition to fluid forces, a virtual disk with propeller characteristics is placed at the stern of the ship model to obtain the response of the hull to fluid and propeller excitations. The virtual disk represents a propeller. It is used when the propeller behaviour is known and the effect of the propeller on the ship hull is to be computed.

In this model, the body force propeller method is applied which models the flow-field interaction between the ship hull and the virtual propeller disk without modelling the full propeller geometry. The flow that is induced by the propeller depends on the flow around the ship hull. Similarly, the hull flow is influenced by the propeller, the propeller performance data (thrust coefficient K_T and the torque coefficient K_Q) are provided as a function of advance ratio J.

3.2.1 Computational grid

For boundary conditions the computational domain used was defined by a box shape satisfying the recommendations of the ((ITTC) International Towing Tank Conference, 2011) procedure (that is, the inlet should be 1-2 L_{PP} and the outlet 3-5 L_{PP}). Table 3 shows the boundary locations for this study and other references.

In this work the ship is studied first with a symmetry plane on the centre line of the hull and second with full geometry (when the virtual disk is applied), including non-slip conditions for the hull wall, and the inlet, top and bottom are taken as velocity inlets with side walls in the positive x

Table 3 Boundaries locations

Reference	Directions				
	Up	Down	Inlet	Outlet	Width
Calm water /Waves	1.25L	2.5L	3L	5.5L	2.5L
(Tezdogan, Demirel, Kellett, Khorasanchi, Incecik, & Turan, 2015)	L	2.3L	2.65L	4.5L	2.5L

Table 4 Grid generation

Total number of Cells	Coarse	Medium	Fine
Calm water	614225	2536761	6714564
Waves	-	2536761	6714564

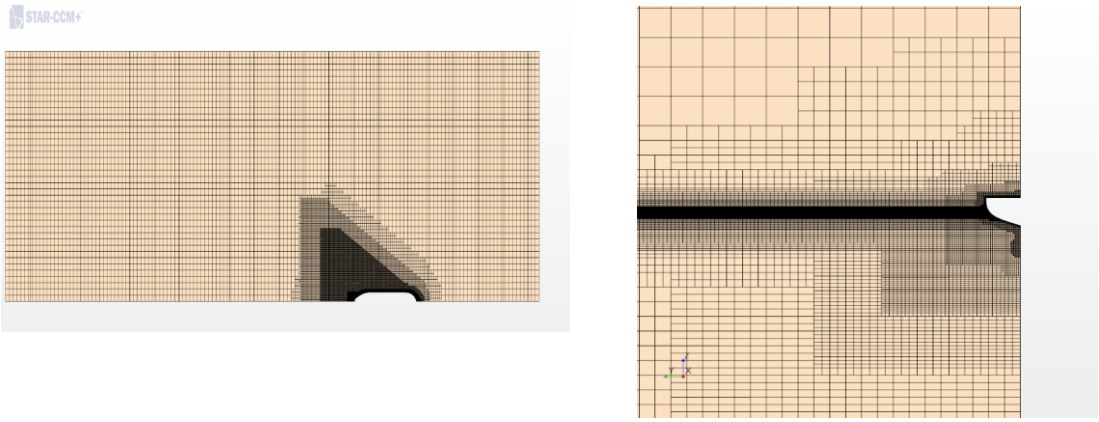

Fig. 2 Mesh generation domain for KVLCC2

Direction. The outlet had a hydrostatic pressure outflow in the negative x direction, in general, these were the boundary conditions taken.

A wave damping of 1L is applied to the outlet and to the side to prevent the appearance of reflected waves. The fluid is considered incompressible, viscous, and non-rotational. Body motions are small in deep water.

The CFD finite volume method was applied to 3-D viscous flows and the mesh generation was based on the hexahedral approach. Automatic meshing offered by STARCCM+ was used for mesh generation with a trimmer surface remesher. Local mesh refinements are permitted due to the hexahedral mesh with volumetric controls around the hull, bulbous bow, stern, around the propeller, and near the free surface.

Three sets of grids are created: a coarse, a medium, and a fine mesh, each with fixed-prism layer thickness. The numerical results in this paper are given for the fine mesh that was limited due to hardware resource limitation shown in Fig. 2, while the grid size is presented in Table 4.

4. Results and discussion

The KVLCC2 ship hull was studied for its design speed of 15.5 Knots, which gives a Froude number (Fr) of 0.142. The time step was calculated according to the ITTC recommendations ((ITTC) International Towing Tank Conference, 2011), which give a range between $\Delta t = 0.005L/U$ and $\Delta t = 0.01L/U$, where: L is the length of the ship and U is the velocity. The time step for this study was 0.05 s. the main work of this paper is the rigid body study, giving ship motions (heave and pitch) and pitch moment as results.

4.1 Total resistance

4.1.1 Total resistance in calm water

Calculation of the total resistance R_T in this study is done by using the formula given by (Tezdogan *et al*. 2015)

$$C_T = \frac{R_T}{0.5\rho A_W U^2} \tag{5}$$

In Eq. (5), A_w is the wetted surface area, ρ is water density, C_T is the total resistance coefficient calculated here as the coefficient of the drag force on x direction. The comparison of the total resistance coefficient from experimental and numerical results in calm water from this study are presented in Table 5.

From the results in Table 5, it is observed that the increase of mesh cells gives more acceptable agreement with the results from experiments. These results were found to be acceptable according to the size of the mesh generated in this study.

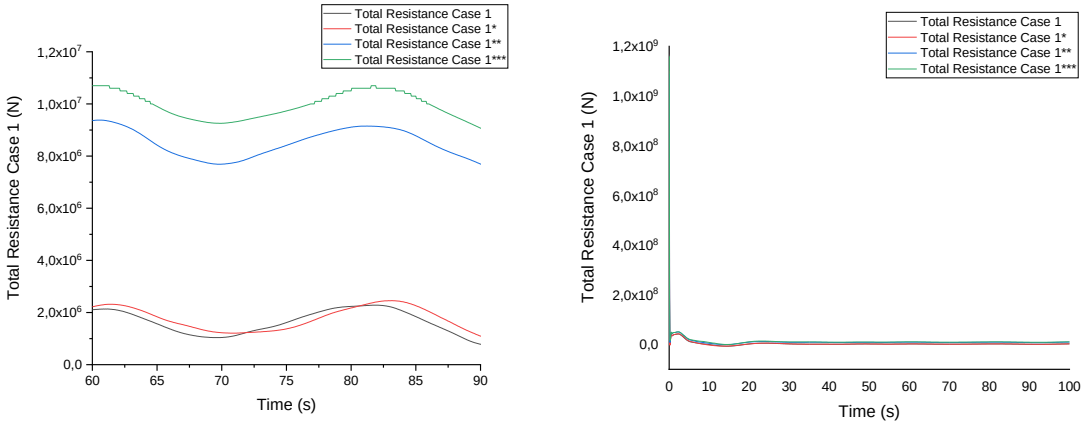

(a) (b)

Fig. 3 Total resistance comparison for different rpm speeds

Table 5 Total resistance coefficient comparison for a speed of 15.5 Knots

	Present work case 1 ($\times 10^{-3}$)	EXP ($\times 10^{-3}$) INSEAN data reported in (Islam *et al.* 2019)	CFD ($\times 10^{-3}$) (Islam *et al.* 2019)
Coarse	2.52	5.14	4.52
Medium	3.02	5.14	-
Fine	4.27	5.14	4.78

Table 6 Propeller dimensions

Propeller N°	KP458	**Propeller name**	KVLCC
Propeller type	FFP	**Designed by**	MOERI
Scale ratio (λ)	58	**Propeller model's diameter**	170 mm
N° of blades	4	A_E/A_0	0.431

Table 7 Propeller power data

J	K_T	$10K_Q$	η_0
0.0000	0.3183	0.3110	0.0000
0.0500	0.3014	0.3032	0.0791
0.1000	0.2843	0.2932	0.1543
0.1500	0.2670	0.2814	0.2265
0.2000	0.2493	0.2682	0.2959
0.2500	0.2315	0.2539	0.3628
0.3000	0.2132	0.2388	0.4263
0.3500	0.1947	0.2230	0.4864
0.4000	0.1757	0.2067	0.5411
0.4500	0.1563	0.1897	0.5901
0.5000	0.1365	0.1721	0.6312
0.5500	0.1161	0.1538	0.6608
0.6000	0.0951	0.1344	0.6757
0.6500	0.0735	0.1138	0.6682
0.7000	0.0511	0.0915	0.6222
0.7500	0.0280	0.0671	0.4981
0.8000	0.0040	0.0402	0.1267

The KVLCC2 hull simulations in calm water are run for case 1, with propeller (defined by a virtual disk), and Fig. 3 shows the results obtained for different propeller velocities. Tables 6 and 7 show the propeller dimensions and specifications and the powering data, respectively.

In this simulation, the KVLCC2 ship is fixed in the x direction. The hull's forward speed is modelled as the ambient fluid relative velocity introduced at the inlet boundary. The thrust induced by the virtual disk model must balance the drag forces on the ship hull, and for this purpose, different rpm were studied (76 rpm, 70 rpm, and 10 rpm); results are shown in Fig. 3. For case 1, the total hull-only

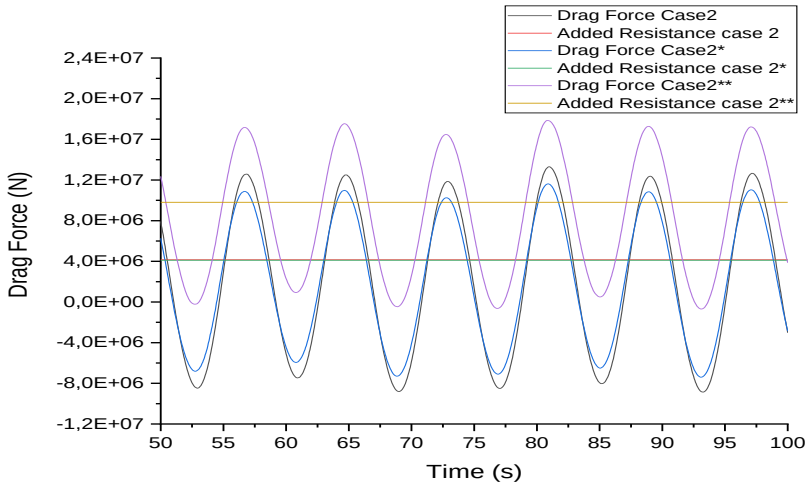

Fig. 4 Added resistance and total Drag force (Case2, 2*, and 2**)

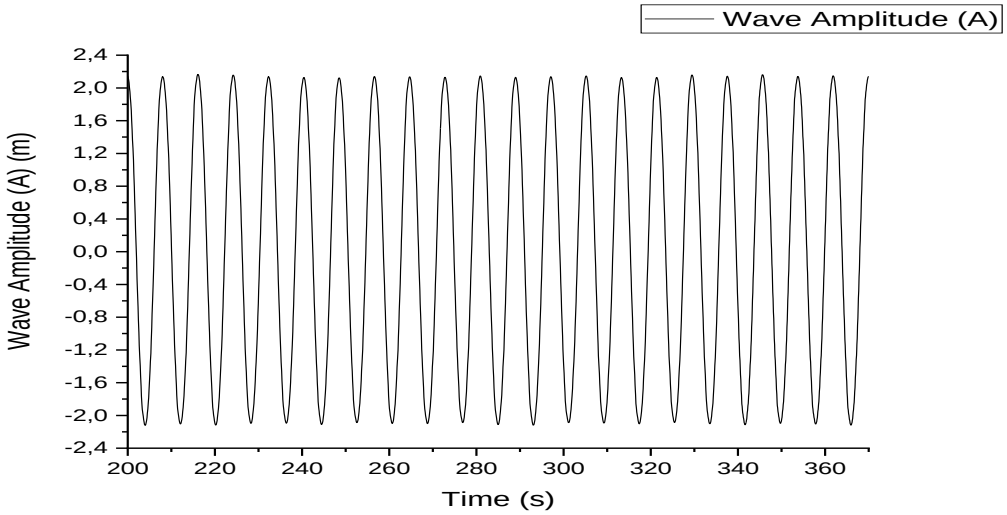

Fig. 5 Time history wave amplitude (Case2)

drag force is shown as black lines and is in agreement with case 1*, whereas for cases 1** and 1*** were not. Note that the colored lines in Fig. 3 (* cases) are the thrust force from the propeller. For the study of the ship in waves (case 2), only two speeds of the virtual disk were investigated (10 rpm and 70 rpm), and the results are presented in the Fig. 4. The results show that the 70 rpm rotational speed of the disk gives a very strong thrust, roughly double the required thrust force to overcome the hull's drag. For the rest of the simulations in waves and for propeller excitations, case 2* is taken as a reference (with 10 rpm). These results confirm that the choice of the 10 rpm for wave study gives acceptable results.

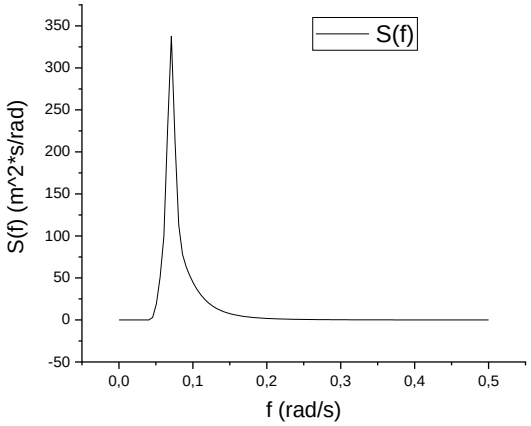

Fig. 6 JONSWAP spectrum (Case5)

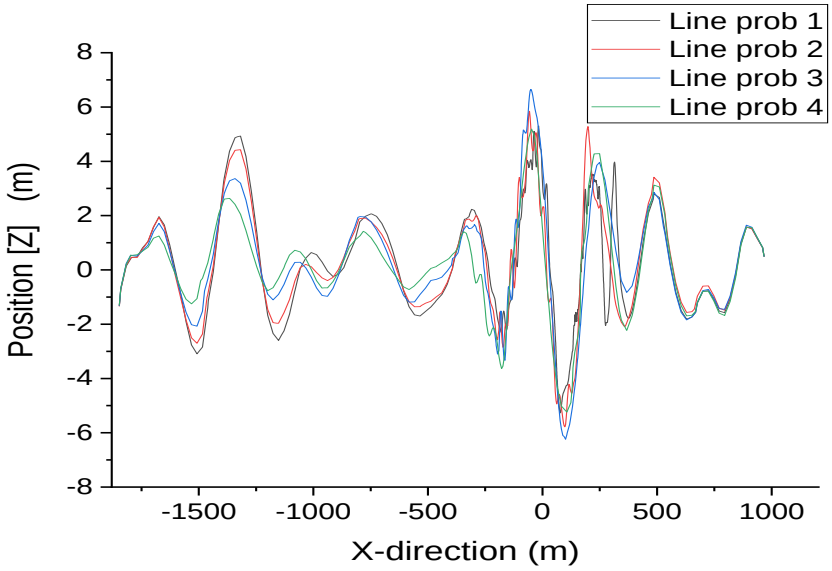

Fig. 7 Time realization of the JONSWAP spectrum at t = 100 s (Case5)

4.1.2 Added resistance in waves

The ship moving in waves faces additional resistance, i.e., added resistance. First, for case 2, waves were run without ship hull (waves only) to monitor the wave generated at the inlet, and the wave amplitude is recorded in front of the ship hull at a distance of 200 m from the inlet. Fig. 5 displays the wave amplitude recorded.

The mean value of the wave amplitude from the Fig. 5 was found to be 2.075 m, while in case 2 the wave amplitude was 2.212 m. This reduction in amplitude was found acceptable after running

the simulation for long period of time. The spectrum of the irregular wave in case 5 is a JONSWAP spectrum that has a peak period of 14.28 s and a significant wave height of 9 m; see Fig. 6.

Four wave probes were used to monitor the wave profile on the KVLCC2 hull and far the field. The positions of these probes are Y/L_{BP} = 0.09375, 0.3125, 0.625, and 0.9375, respectively. These results at the end of the simulation are shown on Fig. 7.

The added resistance increased proportional to the motion, and the maximum recorded added resistance was found in case 4 ($\lambda / L = 1.2$).

Numerical results were compared to the experimental data available from Osaka University and from MOERI, and to the numerical results from (Islam *et al*. 2019), as shown in Fig. 8. From these results, we see that the CFD computation is in good agreement with available experimental data.

Fig. 9 shows a case-by-case comparison of the KVLCC2-hull added resistance with and without a propeller disk. The comparison of the total drag force is also included in the same figure. These figures lead to a conclusion that the presence of virtual propeller disk decreases the added resistance slightly for both regular and irregular waves.

4.2 Ship motion in waves

The ship motion responses are calculated at the centre of gravity of the ship hull. The following formulas were applied for comparison to the experimental data. The heave RAO function is given by

$$\frac{Z}{A} = \frac{Z / L}{A / L} \tag{6}$$

In Eq. (6), Z is the heave amplitude, L is the ship length, and A is the wave amplitude. The pitch RAO function is given by

$$\frac{\theta}{Ak} = \frac{\theta * \lambda / L}{(A / L) * 360} \tag{7}$$

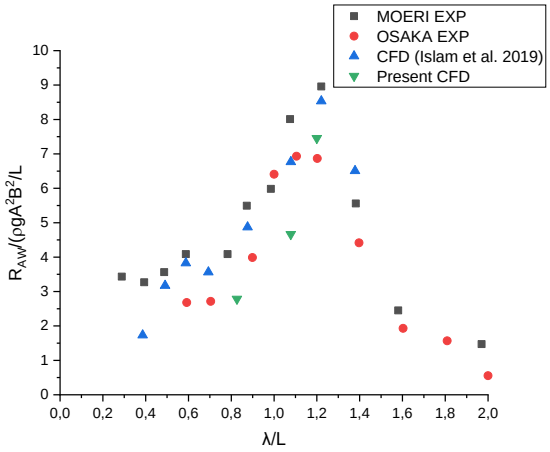

Fig. 8 Added resistance for KVLCC2 (Case2,3, and 4)

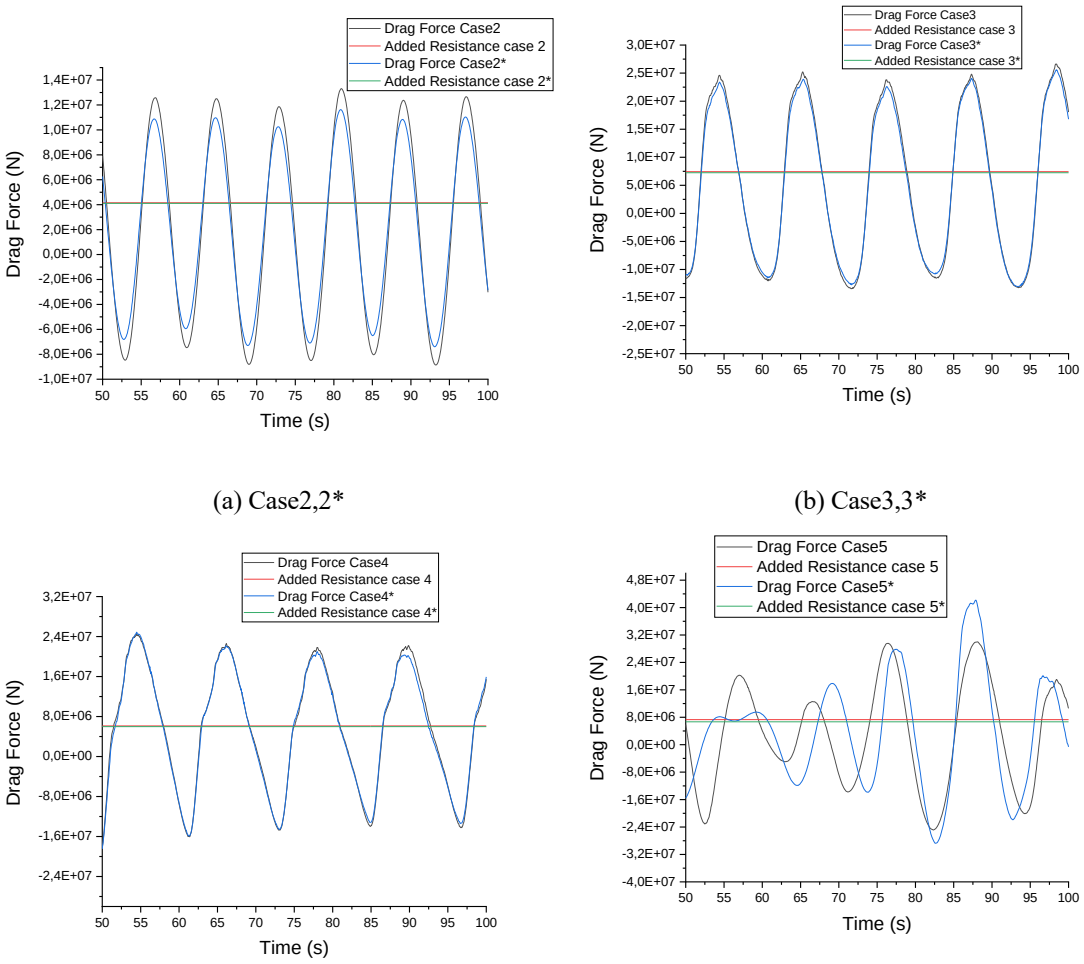

(a) Case2,2* (b) Case3,3*

(c) Case4,4* (d) Case5,5*

Fig. 9 Propeller model effect to the added resistance and total drag force for KVLCC2

In Eq. (7), θ is the pitch amplitude and λ is the wave length.

The heave and pitch motions are compared to the experimental data from MOERI and from Osaka University, and also with the numerical results of (Islam *et al.* 2019), and the results are in agreement, as shown in Figs. 10 and 11.

The heave and pitch time series are shown in Figs. 12 and 13, and the cases for the ship hull with and without a virtual propeller disk are compared.

From these results we see a very small difference for cases 3, 3* and 4, 4*; this difference is acceptable for this study, in contrast to the underestimation for both heave and pitch for cases 2, 2* and 5,5*. The wave in case 2 and 2* induced a difference in results between the case with and without propeller disk. In case 2, the propeller model increases the heave's offset and decreases the

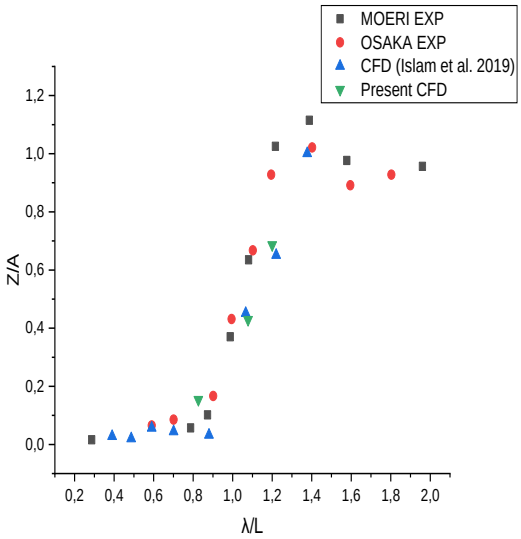

Fig. 10 Heave for KVLCC2 (Case2,3, and 4)

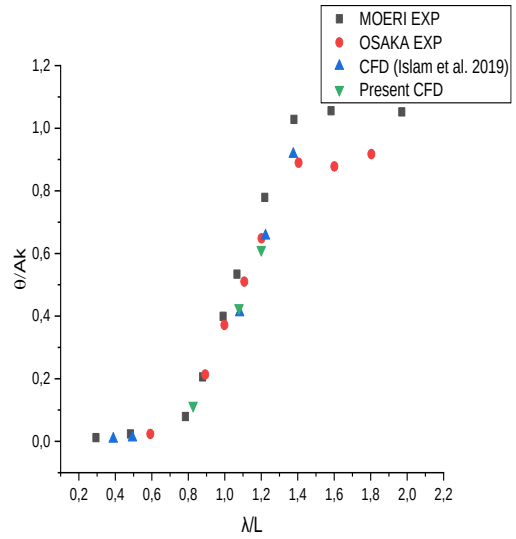

Fig. 11 Pitch for KVLCC2 (Case2,3, and 4)

pitch's offset. However, note that both heave and pitch in case 2 are very small to begin with, almost one magnitude smaller than the other cases. While case 5 and 5* have irregular wave excitation, the results are nevertheless found to be acceptable.

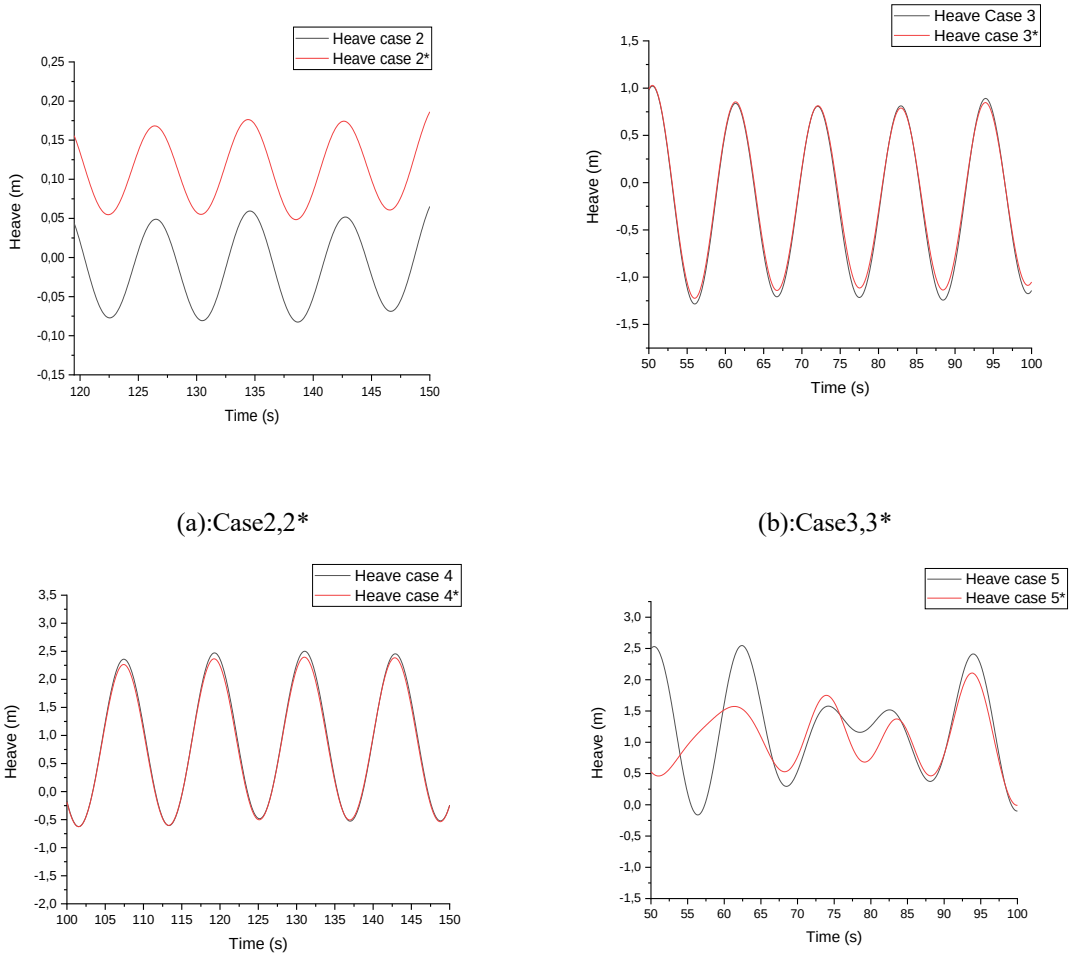

(a):Case2,2* (b):Case3,3*

(c):Case4,4* (d):Case5,5*

Fig. 12 Heave comparison for KVLCC2

4.3 Pitch moment in waves

Results of the pitch moment calculation around the *Y* axis are presented in this section. The wave induced pitch moment results from these cases are shown in Fig. 14, and we see that, for the cases where the hull has a virtual propeller disk, there is increase in excitation forces leading to an increase in the pitch moment response, and the linearity of the response is clear in all cases.

4.4 Wake

The wake of the KVLCC2 hull is studied with a virtual disk propeller model in calm water, and the nominal wake field in the propeller plane is presented in Fig.15 for x = 0.986 m, x = 1.36 m, and x = 1.76 m.

These computational results are in close agreement with the results of (Win *et al*. 2016), and the behaviour is similar. This makes the virtual disk a very good choice for calculations since it minimises the mesh and it does not require any geometrical or separate region creation for modelling the propeller behind the ship. Hence this virtual disk is considered more straightforward.

5. Conclusions

STAR CCM+ commercial software was used to study the dynamic response of the KVLCC2 hull in calm water, with regular or irregular waves, based on the DFBI model and RANS approach. The prediction of the total resistance in calm water, added resistance in waves, ship motions, and pitch moment at a ship velocity of 15.5 Knots is presented.

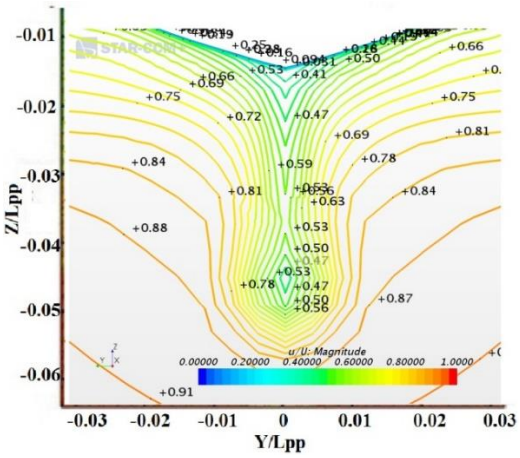

(a) Nominal wake at propeller plane x=1.36 m

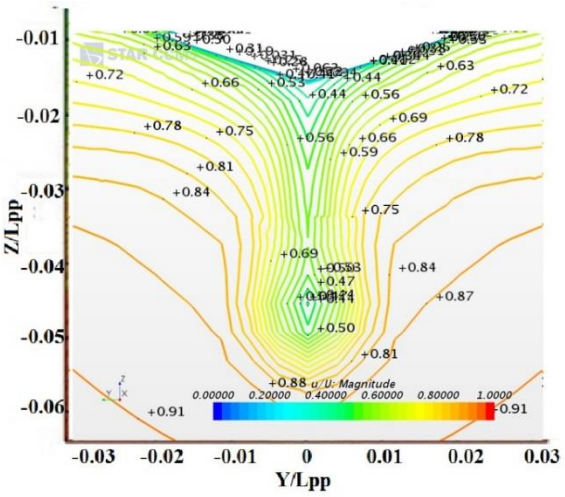

(b) Nominal wake at propeller plane x=1.76 m

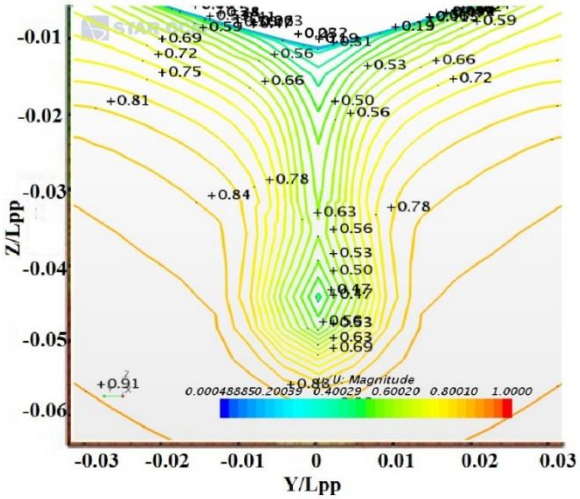

(c) Nominal wake at propeller plane x=0.986 m

Continued-

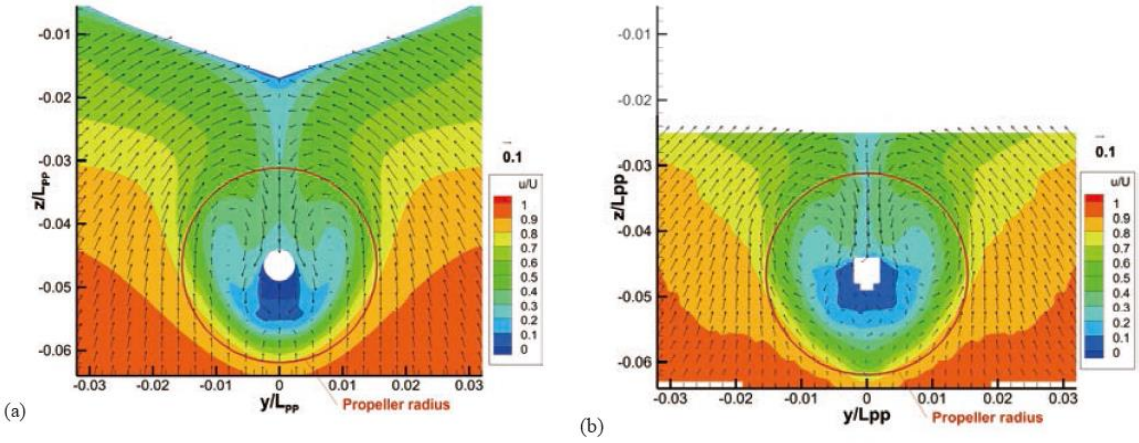

Wave flow field at the propeller plane X=0.98 for CFD (Win *et al*. 2016)

Wave flow field at the propeller plane X=0.98 for PIV (Win *et al*. 2016)

Fig. 15 Wake flow field comparison

Numerical results for the total ship resistance and added resistance in waves of the KVLCC2 hull are in good agreement with previous experimental and numerical research; ship motions (heave and pitch responses) for both regular and irregular waves were also in good agreement, lending support to the CFD techniques used in this approach.

The ship hull is studied with and without a virtual disk propeller that has the same characteristics as a propeller designed for the KVLCC2 but not included geometrically in the model. The results are discussed and compared to the experimental and numerical data. The ship's global response and loading is shown to be affected by the introduction of the virtual disk propeller, especially the ship's pitch moment. The use of a virtual disk is suitable for speeding up the computations, knowing that the propeller geometry is designed but not presented in the model, which makes for fewer meshing elements and less refinement at the boundaries. This virtual disk model has proved its efficiency and straightforwardness.

References

An, N.H., Ryu, S.H., Chun, H.H. and Lee, I. (2014), "An experimental assessement of resistance reduction and wake modification of KVLCC model by using outer-layer vertical blades", *Int. J. Nav. Archit. Ocean Eng*., **6**, 151-161.

Barhoumi, M. and Storhaug, G. (2014), "Assessment of whipping and springing on a large container vessel", *Int. J. Nav. Archit. Ocean Eng*., **6**, 442-458.

Hong, S.Y. and Kim, B.W. (2014), "Experimental investigations of higher-order springing and whipping-WILS project", *Int. J. Nav. Archit. Ocean Eng*., **6**, 1160-1181.

International Towing Tank Conference. (ITTC) (2011), Practical guidelines for ship CFD applications.

Islam, H., Rahaman, M.M. and Akimoto, H. (2019), "Added Resistance Prediction of KVLCC2 in Oblique Waves", *Am. J. Fluid Dynam.*, **9**(1), 13-26.

Kim, J.H. and Kim, Y. (2014), "Numerical analysis on springing and whipping using fully-coupled", *Ocean Eng*., **91**, 28-50.

Kim, J.H., Kim, Y. and Korobkin, A. (2014), "Comparison of fully coupled hydroelastic computation and segmented model test results for slamming and whipping loads", *Int. J. Nav. Archit. Ocean Eng*., **6**, 1064-1081.

Kim, M., Hizir, O., Turan, O. and Incecik, A. (2017), "Numerical studies on added resistance and motions of KVLCC2 in head seas for various ship speeds", *Ocean Eng*., **140**, 466-476.

Kim, Y. and Kim, J.H. (2016), "Benchmark study on motions and loads of a 6750-TEU containership", *Ocean Eng.*, **119**, 262-273.

Lakshmynarayanana, P., Temarel, P. and Chen, Z. (2015), "Coupled Fluid-Structure Interaction to model Three-Dimentional Dynamic Behaviour of Ship in Waves", *Proceedings of the 7th International Conference on Hydroelasticity in Marine Technology.* Split, Croatia.

Larsson, L. and Raven, H.C. (2010), Shio resistance and flow, In R.H. Larsson L, *THE PRINCIPLES OF NAVAL ARCHITECTURE SERIES.* The Society of Naval Architects and Marine Engineers, USA.

Seng, S., Jensen, J.J. and Malenica, Š. (2014), "Global hydroelastic model for springing and whipping based on a free-surface CFD code (OpenFOAM)", *Int. J. Nav. Archit. Ocean Eng*., **6**, 1024-1040.

Storhaug, G. (2014), "The measured contribution of whipping and springing on the fatigue and extreme loading of container vessels", *Int. J. Nav. Archit. Ocean Eng*., **6**, 1096-1110.

Tezdogan, T., Demirel, Y.K., Kellett, P., Khorasanchi, M., Incecik, A. and Turan, O. (2015), "Full-scale unsteady RANS CFD simulations of ship behaviour and performance in head seas due to slow steaming", *Ocean Eng*., **97**, 186-206.

Win, Y.N., Akamatsu, K., Stern, F., Wu, P.C., Okawa, H. and Toda, Y. (2016), *RANS Simulation of KVLCC2 using Simple Body-Force Propeller Model With Rudder and Without Rudder.*

MK

Nomenclature

u, v, w	Velocity components
ρ	Density
τ_{ij}	Stress tensor
μ_T	Turbulent dynamic viscosity
M	Mass matrix
K	Stiffness matrix
$\dot{\vec{X}}(t)$	Velocity vector
$\vec{F}(t)$	External forces vector
U	Ship speed
C_T	Total resistance coefficient
p	Mean pressure
g	Acceleration due to gravity
μ	Dynamic viscosity
k	Turbulent kinetic energy
C	Damping matrix
$\vec{X}(t)$	Displacement vector
$\ddot{\vec{X}}(t)$	Acceleration vector
L	Length between perpendiculars
R_T	Total ship resistance